ELSEVIER

Contents lists available at ScienceDirect

# Electric Power Systems Research

journal homepage: www.elsevier.com/locate/epsr



# Observations of very unusual behavior of lightning discharges

Z. Ding\*, V.A. Rakov

Department of Electrical and Computer Engineering, University of Florida, Gainesville, FL, USA

### ARTICLE INFO

# Keywords: Lightning discharge Negative lightning Positive lightning Bipolar lightning Hybrid lightning Multiple ground terminations High-Speed optical imaging Visible Infrared Ultraviolet Electric field waveforms

### ABSTRACT

Based on recent observations at the Lightning Observatory in Gainesville (LOG), Florida, we present three examples of very unusual behavior of cloud-to-ground (CG) lightning flashes: (a) One +CG and one towerterminated -CG separated by 11 km, were briefly coupled, so that positive charge was in effect drawn from the ground at the position of -CG and injected into the ground at the position of +CG. That unusual interaction was accomplished by the initiation of M-component incident wave in the +CG channel by the leader of the first stroke of the -CG. (b) A branched positive leader intermittently extended via bidirectional transients separated by inactive intervals of about 5 ms, on average. One of the bidirectional transients, moving negative charge in the backward direction, triggered a downward negative leader, resulting in a three-stroke -CG. (c) A subsequent-stroke negative leader, moving through virgin air, entered the lower part of residual (non-luminous) first-stroke channel, in addition to creating a new ground termination about 950 m away. Studying unusual lightning behavior helps to improve our understanding of the variability of basic lightning processes and to identify new potential lightning hazards to various objects and systems.

## 1. Introduction

There has been considerable progress in improving our understanding of lightning behavior, which is mostly based on the wide use of high-speed framing cameras (e.g., Saba et al., [1,2], Warner et al., [3], Tran and Rakov, [4,5], Visacro et al., [6,7], Ding et al., [8,9], Nag et al., [10], B. Wu et al., [11,12]), VHF source mapping systems (e.g., Rison et al., [13], Stock et al., [14], van der Velde et al., [15], Jiang et al., [16, 17], Hare et al., [18], Pu et al., [19], Jensen et al., [20], or both (e.g., Yuan et al., [21,22], Jiang et al., [23])). In this paper, we present recent observations of very unusual lightning behavior including: (a) the ability of negative cloud-to-ground discharge (+CG) to talk to a concurrent positive cloud-to-ground discharge (-CG) many kilometers away, (b) the ability of downward positive leader to produce an opposite-polarity (negative) lightning discharge to ground (-CG), and (c) the ability of downward negative leader branch to enter the residual (non-luminous) channel of the preceding stroke at a height of some tens of meters above the ground surface, in addition to its other branch creating a new ground termination point. The paper is based on (is an extended version of) the Keynote Speech given by the authors at the GROUND 2023 & 10th LPE in Belo Horizonte, Brazil.

Studying and documenting unusual or less common lightning behavior helps to improve our understanding of the variability of basic

lightning processes and to identify new potential lightning hazards to various objects and systems.

# 2. Instrumentation

All data presented in this paper were acquired at the Lightning Observatory in Gainesville (LOG), Florida, which is equipped with multiple high-speed framing cameras, wideband electric and magnetic field measuring systems, and X-ray/gamma-ray detectors. The LOG instrumentation (GPS-synchronized) used in this study was set to trigger on electric field changes produced by close lightning (within about 6 km of LOG). U.S. National Lightning Detection Network (NLDN) data were used to determine the distances to lightning channels and obtain estimates of return-stroke peak currents. The mean location error of NLDN after the 2013 upgrade in Florida is estimated to be 146 m [24].

The high-speed framing cameras used in this study included Phantom V310 (visible range;  $0.4-0.8~\mu m$ ) and FLIR X6900sc (medium-to-far infrared (IR) range;  $3.0-5.0~\mu m$ ). We additionally used a Corona-Finder UV intensifier coupled with a U-340 filter and a Phantom v711 framing camera to obtain lightning images in the ultra-violet (UV) range; 290-370~n m. UV images of lightning have never been reported before. The Phantom v310 camera had resolution of  $288\times512~pixels$  and was operated at 20,000 fps (frames per second) with  $47.39~\mu s$ 

E-mail addresses: ziqinding94@ufl.edu (Z. Ding), rakov@ece.ufl.edu (V.A. Rakov).

<sup>\*</sup> Corresponding authors.

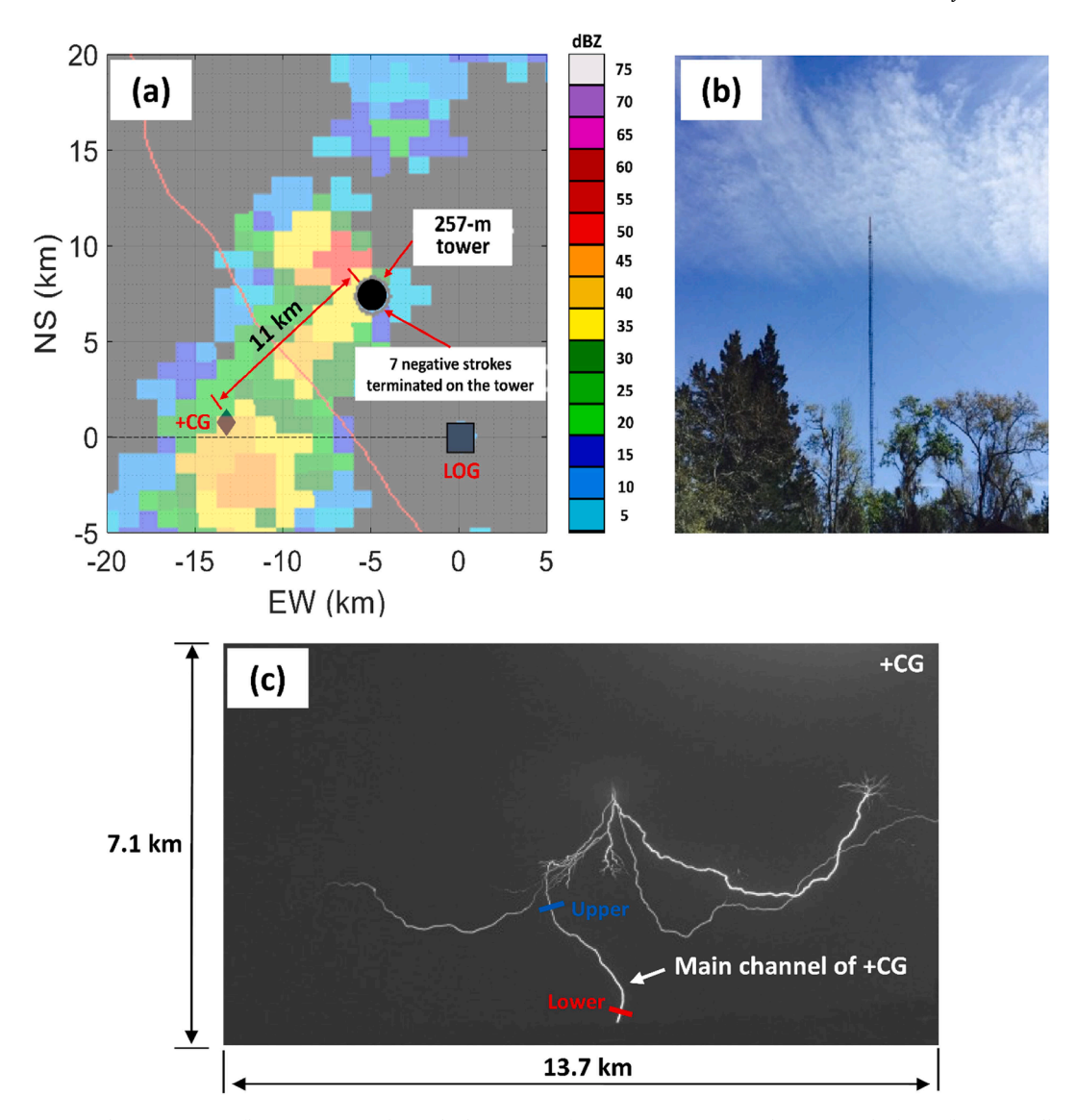


Fig. 1. Flash Z1906. (a) Radar composite reflectivity map with overlaid positions of +CG, 257-m tower, and LOG. Two higher-reflectivity cells are schematically shown in cartoons presented in Figs. 4c and d and in Fig. A1. Distances from LOG to +CG and 257-m tower are 13 km and 8.8 km, respectively. (b) Photo of the 257-m tower. (c) Visible-range composite image of 6000 unsaturated frames after the onset of the RS stage of +CG. The radar data were obtained from the radar station located in Jacksonville, Florida (https://www.ncdc.noaa.gov/nexradiny/chooseday.jsp?id=kjax).

exposure time and 2.61  $\mu s$  dead time. The FLIR camera was operated at 1004 fps with 0.8 ms exposure time and 196  $\mu s$  dead time. Its resolution was 640  $\times$  512 pixels. The UV system was operated at 49,000 fps with 19.81  $\mu s$  exposure time and 600 ns dead time. Its resolution was 368  $\times$  320 pixels. In this paper, we refer to FLIR, Phantom v310, and UV system frames as 1-ms, 50- $\mu s$ , and 20- $\mu s$  frames, respectively. Information about our imaging systems is also tabulated below. Flash Z1906, presented in Section 3.1, was recorded by the Phantom v310 camera, Flash Z2002, presented in Section 3.2, was recorded by the Phantom v310 and FLIR cameras, and Flash Z2004 was recorded by all three imaging systems (in the visible, IR, and UV ranges). All distances and channel extension speeds presented in this paper are 2D.

Four types of radiofrequency field records were used in this study: low-gain E-field records with an instrumental decay time constant of 10 ms, high-gain E-field records with an instrumental decay time constant of 440  $\mu s$ , electric field derivative (dE/dt), and magnetic field derivative (dB/dt) records. The upper frequency response (-3 dB) for both the low-gain and the high-gain E-field measuring systems was 12.5 MHz. In all the electric field waveforms shown in this paper (see Section 3.1), we use the physics sign convention [e.g., Rakov and Uman (2003, section 1.4.2) [25]], according to which the negative return-stroke electric field change is negative.

The luminosity variation measurements presented in this paper are based on the high-speed camera images. The procedure was as follows.

Imaging System	Wavelength (μm)	Framing Rate (fps)	Resolution (pixels)	Exposure Time (μs)	Dead Time (μs)	Interframe Interval (μs)
Phantom v310 (Visible range) FLIR X6900sc (Medium-to-far infrared range)	0.4 - 0.8 3 - 5	20,000 1004	288 × 512 640 × 512	47.39 800	2.61 196	50 1000
CoronaFinder UV intensifier + Phantom v711 (Ultraviolet range)	0.29 – 0.37	49,000	368 × 320	19.81	0.6	20

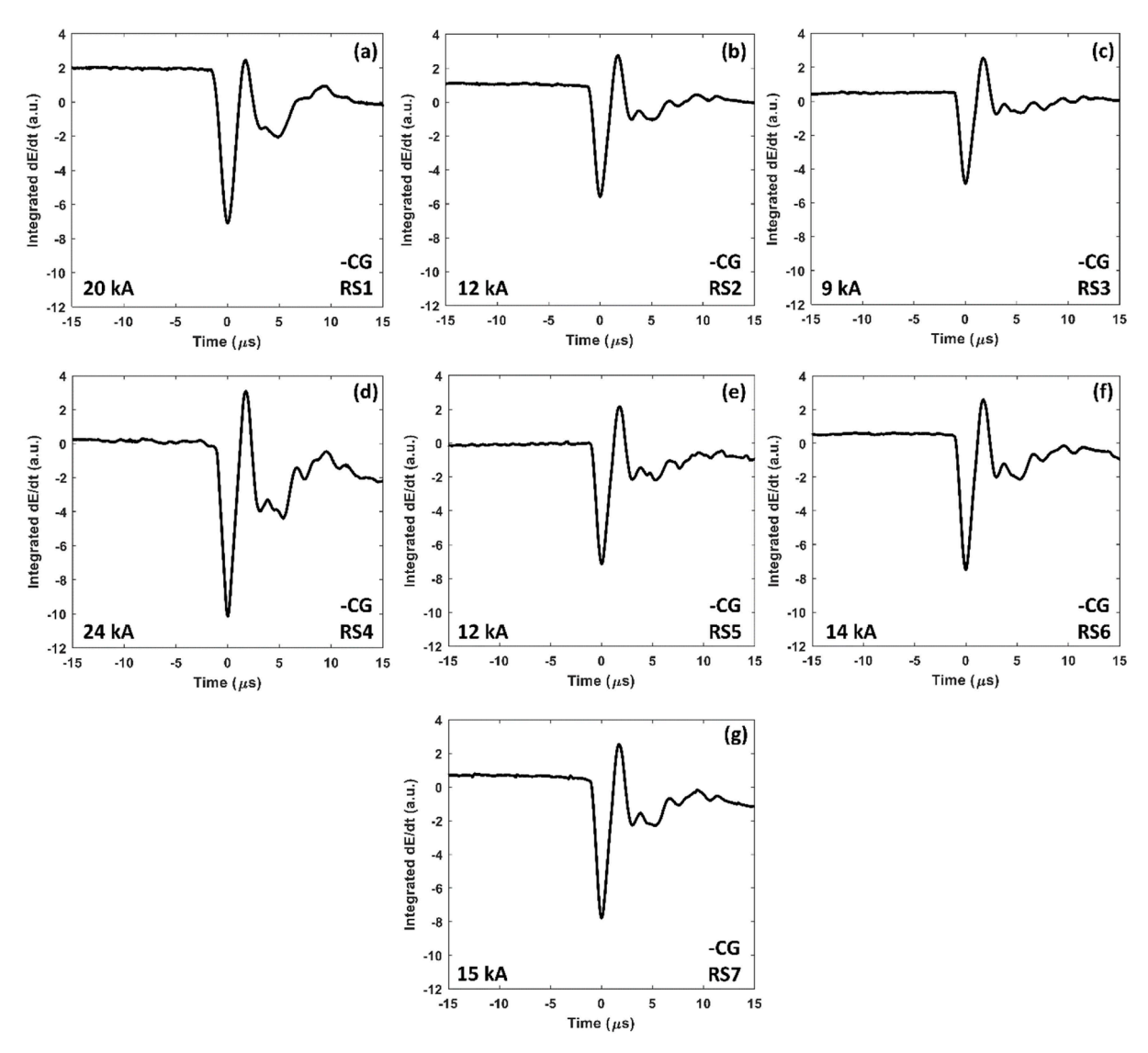


Fig. 2. Flash Z1906. E-field waveforms (physics sign convention) of seven return strokes (RSs) of the 257-m-tower-terminated -CG which was concurrent with the +CG 11 km away (see Fig. 1). The waveforms were obtained by integrating dE/dt waveforms recorded at LOG, 8.8 km from the tower. RS1 and RS2 occurred during the 50-ms long CC stage of the +CG, and RS1 was coincident with the M-component in the +CG main channel (see Fig. 1c). All the E-field waveforms exhibit early zero-crossings (initial half-cycles are as short 3 µs or so) and oscillations, these features being "fingerprints" of lightning strikes to tall towers (Zhu et al., 2018 [31]). Since all the leader/RS E-field waveforms were characteristic of subsequent strokes, we inferred that the tower flash (-CG) was of upward type.

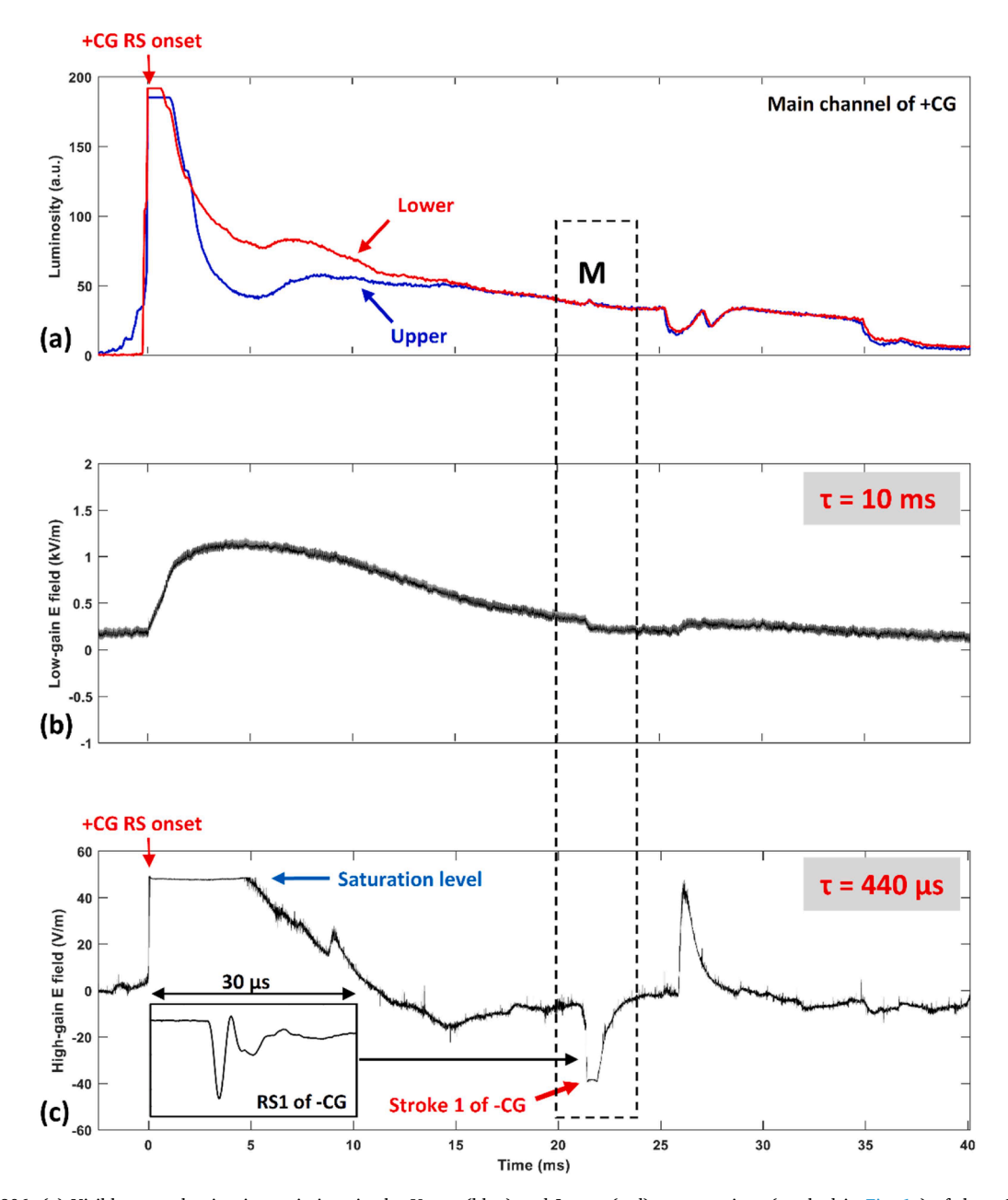


Fig. 3. Flash Z1906. (a) Visible-range luminosity variations in the Upper (blue) and Lower (red) cross-sections (marked in Fig. 1c) of the +CG main channel, including M-component labeled M. (b) and (c) Low-gain and high-gain electric field waveforms, respectively, aligned with the luminosity variations shown in (a). Full timescale is 42 ms and the alignment uncertainty is  $\pm 12.5 \,\mu s$ . Note that the luminosity signature of M-component in the +CG main channel seen in (a) is essentially coincident with the electric field signature of Stroke 1 of -CG in (c). Those two signatures (inside the dashed-line rectangular box) are shown on an expanded (4 ms) time scale in Fig. 4. Inset in (c) shows, on a 30- $\mu s$  timescale, the integrated dE/dt waveform for the RS stage of Stroke 1 of the -CG. Adapted from Ding et al. [32].

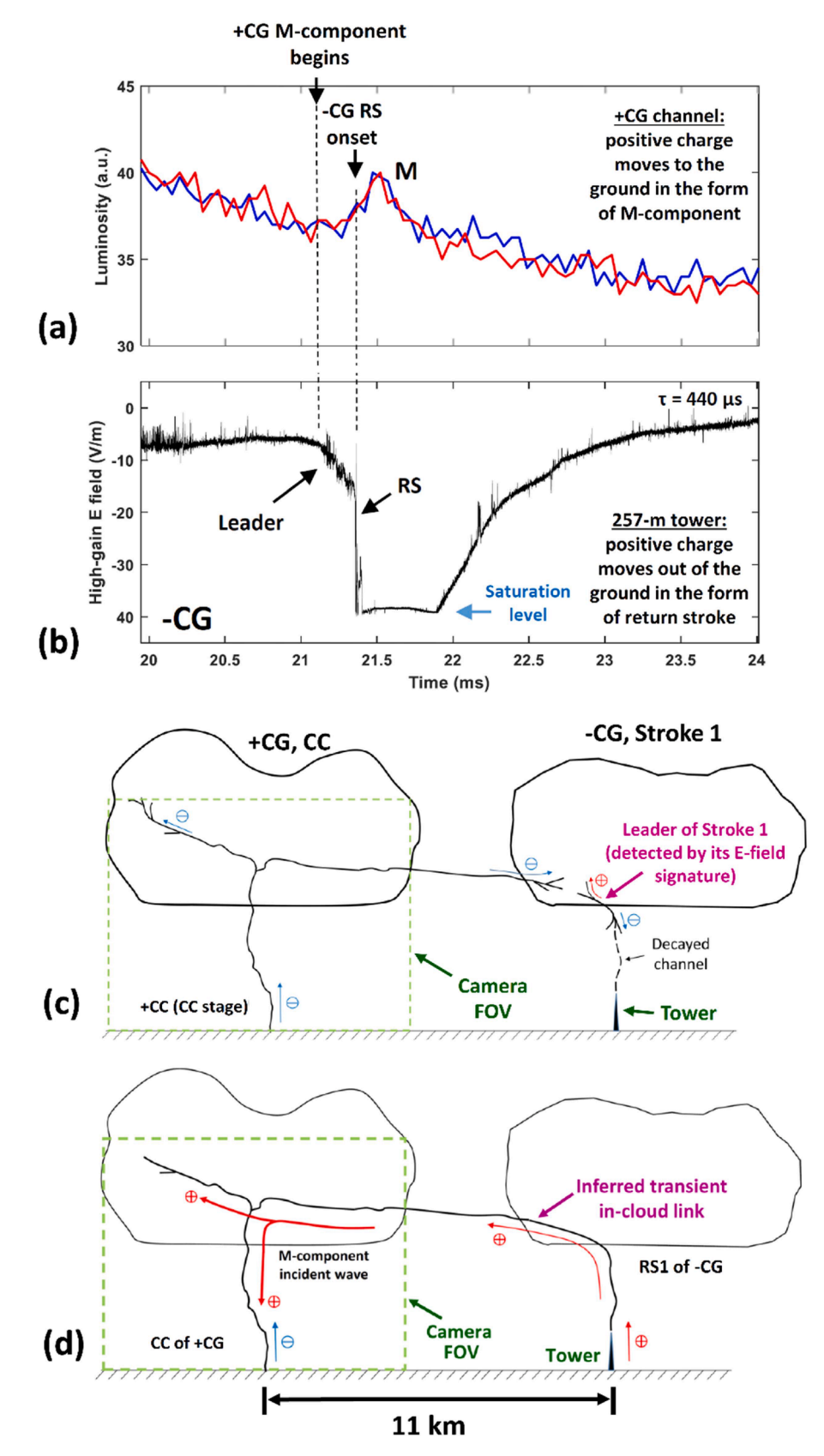


Fig. 4. Flash Z1906. (a) and (b) Expansions of (a) and (c) in Fig. 3, respectively, showing the signatures of M-component in the +CG and Stroke 1 in the -CG displayed on a 4-ms timescale. Alignment uncertainty is  $\pm 12.5 \,\mu s$ . The +CG RS onset signifies the movement of positive charge from the ground to the cloud at the position of the tower, occurring at the same time as the positive charge is moving to the ground in the form of M-component at the position of +CG channel. (c) and (d) Schematic diagrams illustrating a possible mechanism of this unusual lightning behavior.

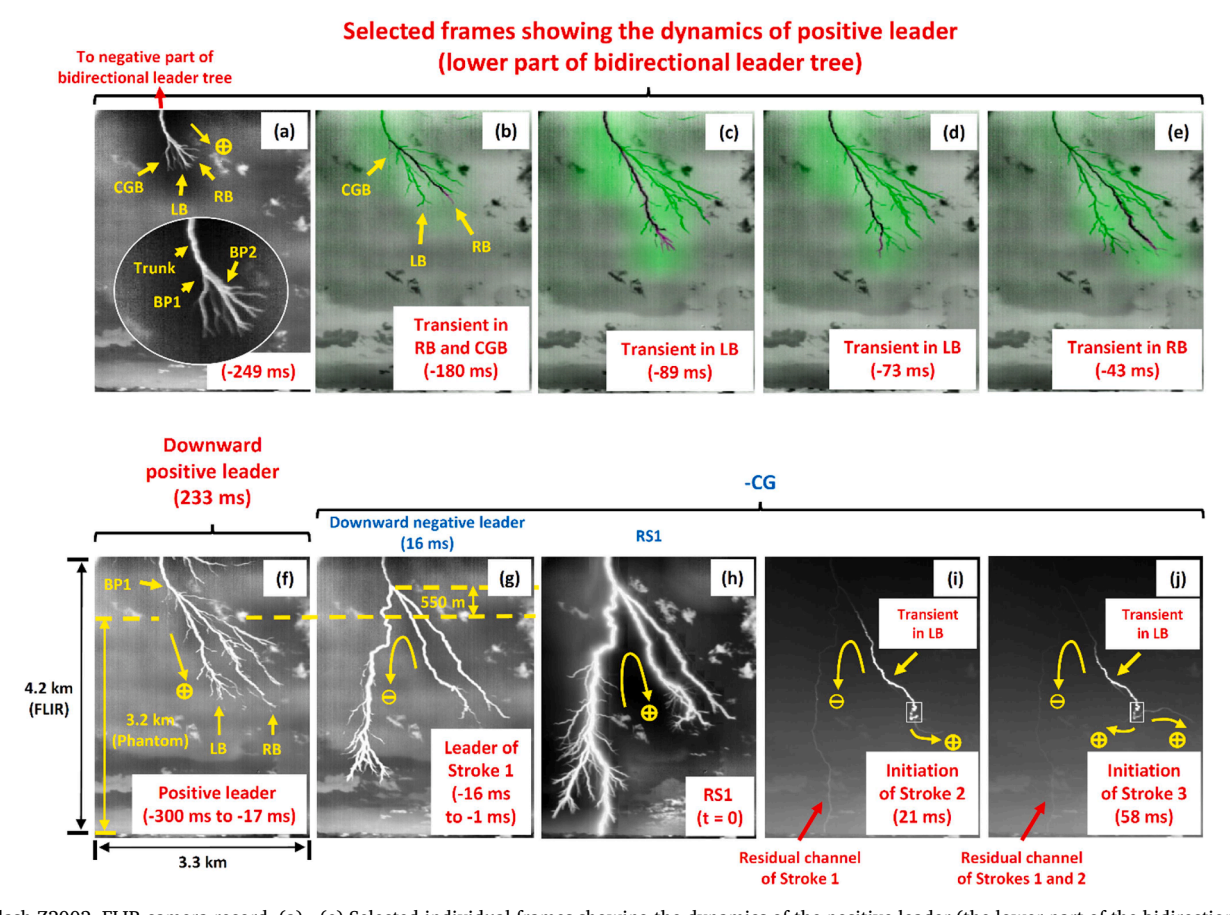


Fig. 5. Flash Z2002. FLIR camera record. (a) - (e) Selected individual frames showing the dynamics of the positive leader (the lower part of the bidirectional leader tree, the upper (negative) part of which is outside of the FOV). Times are given relative to the first RS (RS1) of -CG. The green color in (b) - (e) represents the composite of all the preceding frames, the magenta color represents the process newly imaged in a given frame and not following any previously created (detectable) channel, and the black color represents superposition of magenta on green. (f) Composite image of 283 individual frames (Frame -300 to Frame -17; frame number is also the number of milliseconds before RS1) showing the positive leader just prior to the initiation of -CG. (g) Composite image of 16 individual frames (Frame -16 to Frame -1) showing the stepped leader of Stroke 1 of -CG. (h) Single frame (t = 0) showing RS1 of -CG. (i) and (j) Frame 21 and Frame 58 showing initiation of Strokes 2 and 3, respectively, with IR (elevated-temperature, but not luminous in the visible range) images of residual channels of the preceding stroke(s) being also visible in both cases. The small white boxes in (i) and (j) enclose the initiation regions as seen in the Phantom record (not shown here). BP stands for branching point. Between Frames -249 and -17, over a time interval of 232 ms, branches labeled LB and RB extended by 1480 and 2070 m with overall speeds of  $7.5 \times 10^3$  and  $9 \times 10^3$  m/s, respectively. The interframe interval is 1-ms.

The cross-sections are selected to be perpendicular to the lightning channel section of interest. The luminosity of the cross-section is calculated as the mean value of all pixels above certain threshold that are intersected by the cross-section line. The luminosity threshold was determined by examining the background luminosity of the frame in question and set to the maximum value of the mean values found for several regions of the frame away from the lightning image area. The background luminosity was subtracted from the luminosity of the cross-section.

More detailed information on LOG and its instrumentation can be found in the review papers by Rakov et al. ([26,27,28]) and Ding and Rakov [29].

# 3. Observations, analysis, and discussion

# 3.1. Case 1, flash Z1906: brief electric coupling between concurrent +CG and -CG

Flash Z1906 occurred on July 9th, 2019 at 20:42:21.3276299 UTC and was initially identified as a single-stroke +CG. According to the U.S. National Lightning Detection Network (NLDN), it attached to ground at a distance of 13 km from LOG, and its return-stroke peak current was 95

kA. Later, via detailed analysis of all the available data, we discovered that this +CG was concurrent with a seven-stroke -CG located 11 km away from the +CG main channel (see Fig. 1).

The +CG return stroke (RS) was followed by a continuing current (CC) of about 50 ms in duration, estimated from both optical and electric field records. All seven strokes of the -CG terminated on the 257-m tall tower, located 8.8 km from LOG. The -CG channel was outside of the field of view of the cameras installed at LOG, and its termination on the 257-m tower was established using NLDN data and the previously identified (Zhu et al., 2017 [30], 2018 [31]) characteristic RS E-field signatures (showing early zero-crossing and oscillatory tail), based on observations with the same instrumentation and for the same tower. Electric field waveforms, obtained by integrating the measured dE/dt waveforms, for all seven return strokes of the -CG are shown in Fig. 2. RS1 and RS2 occurred during the CC stage of the +CG, and RS1 was coincident with the M-component (luminosity surge in the +CG main channel).

In order to show the context in which RS1 of –CG and the M-component of +CG occurred, we show in Fig. 3 the optical and E-field data on a 42-ms scale, aligned with an uncertainty of  $\pm 12.5~\mu s$ . Both the –CG RS1 and the +CG M-component are shown on an expanded, 4-ms, time scale, along with schematic diagrams (cartoons) illustrating a

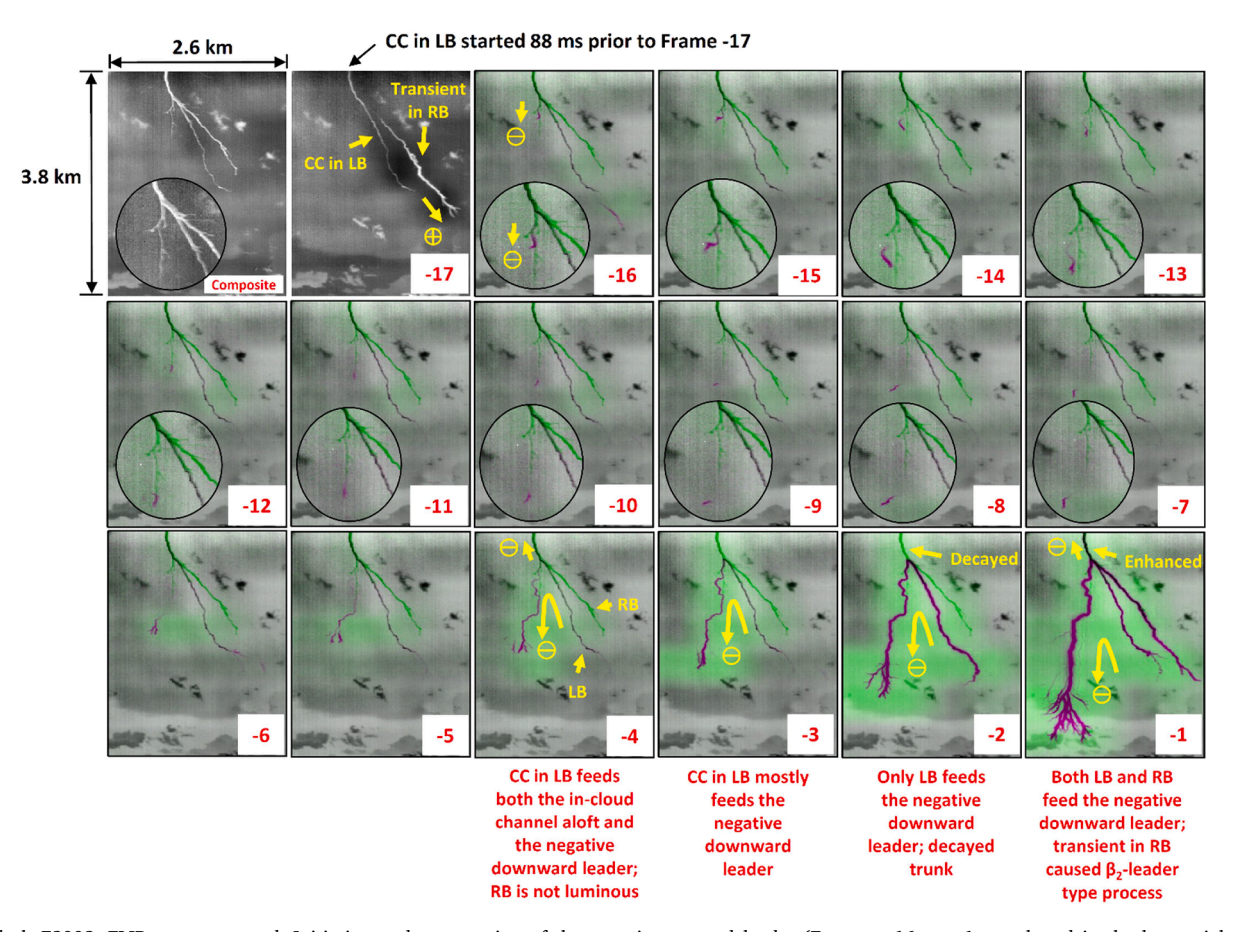


Fig. 6. Flash Z2002. FLIR camera record. Initiation and propagation of the negative stepped leader (Frames -16 to -1, numbered in the lower-right corner) preceded by the transient in branch RB seen in Frame -17. The frame numbers also represent the number of milliseconds prior to the RS1 onset. In Frames -16 to -1, the green color represents the composite of six preceding frames (Frames -258, -249, -238, -180, -86, and -26), shown in black-and-white in the upper-left corner of this figure. Those six frames were selected to show all the main branches involved. The magenta color in Frames -16 to -1 represents the process newly imaged in a given frame and not following any previously created channel seen in the composite image, and the black color represents the superposition of magenta on green. Note that branch LB is continuously luminous in all the individual frames shown here, while branch RB exhibits significant luminosity only in individual Frames -17 and -1.

possible mechanism of their occurrence.

At the time of the M-component, NLDN (also the Earth Networks Total Lightning Network, ENTLN) reported a negative stroke terminated on the 257-m tower, which was outside of the field of view of the cameras operating at LOG and 11 km away from the +CG main channel seen in Fig. 1c. This negative stroke (Stroke 1 of the seven-stroke towerterminated -CG) apparently caused the M-component labeled M in Figs. 3a and 4a, which implies the presence of an in-cloud link between them. There were no M-components in the +CG main channel associated with the other six return strokes of the tower-terminated -CG, which suggests that the inferred coupling between the tower and the +CG channel was brief. Based on the time coincidence of the M-component in the main channel of the +CG (see Fig. 4a) and the electric field signature characteristic of negative RS terminated on the 257-m tower (see Fig. 4b), we conclude that there was electric coupling between the +CG and the -CG, such that the electric charge was in effect transferred, via an inferred transient in-cloud link, between the two points on the ground separated by 11 km. The inferred in-cloud link must have existed before the -CG RS onset in order to explain the observations described above; in the absence of such link, there would have been an appreciable delay between the M-component and RS waveforms (an in-cloud leader propagating at a speed of 10<sup>6</sup> m/s would need 11 ms to cover the 11-km distance separating the tower and the +CG channel), not seen in Fig. 4a and b. Further, it appears that the M-component in the +CG channel

begins about 250  $\mu$ s ( $\pm 12.5 \mu$ s which is our alignment uncertainty) prior to the -CG RS onset (M-component and RS onset times are marked by vertical dashed lines in Fig. 4a and b), which implies that the inferred incloud link between the -CG and +CG channels to ground was established during the leader stage of Stroke 1 of the -CG. In other words, the downward negative leader above the tower was draining (at least in part) negative charge from the ground via the +CG channel 11 km away and the inferred in-cloud link. It is worth noting that the distances from LOG to the +CG main channel and to the tower are different, 13 and 8.8 km, respectively. This difference in distances corresponds a difference in propagation times of electromagnetic signals in air of 14 µs. Accounting for this difference in propagation times to LOG, would lead to a larger delay of the RS onset in the -CG relative to the M-component onset in the +CG, which further supports our inference that electrical connection between the +CG and -CG was established during the leader stage of Stroke 1 of the -CG (see Fig. 4c and d). A more detailed hypothetical scenario leading to establishment of a transient in-cloud link between the +CG main channel and the tower-terminated Stroke 1 of the -CG is schematically shown in Fig. A1.

The tower-terminated -CG was likely an upward flash, since all its strokes were of subsequent-stroke type (see Fig. 2). An upward flash initiated from the same tower was previously observed at LOG by Zhu et al. [4], who used both a high-speed framing camera and an electric field measuring system. They presented optical evidence that all strokes

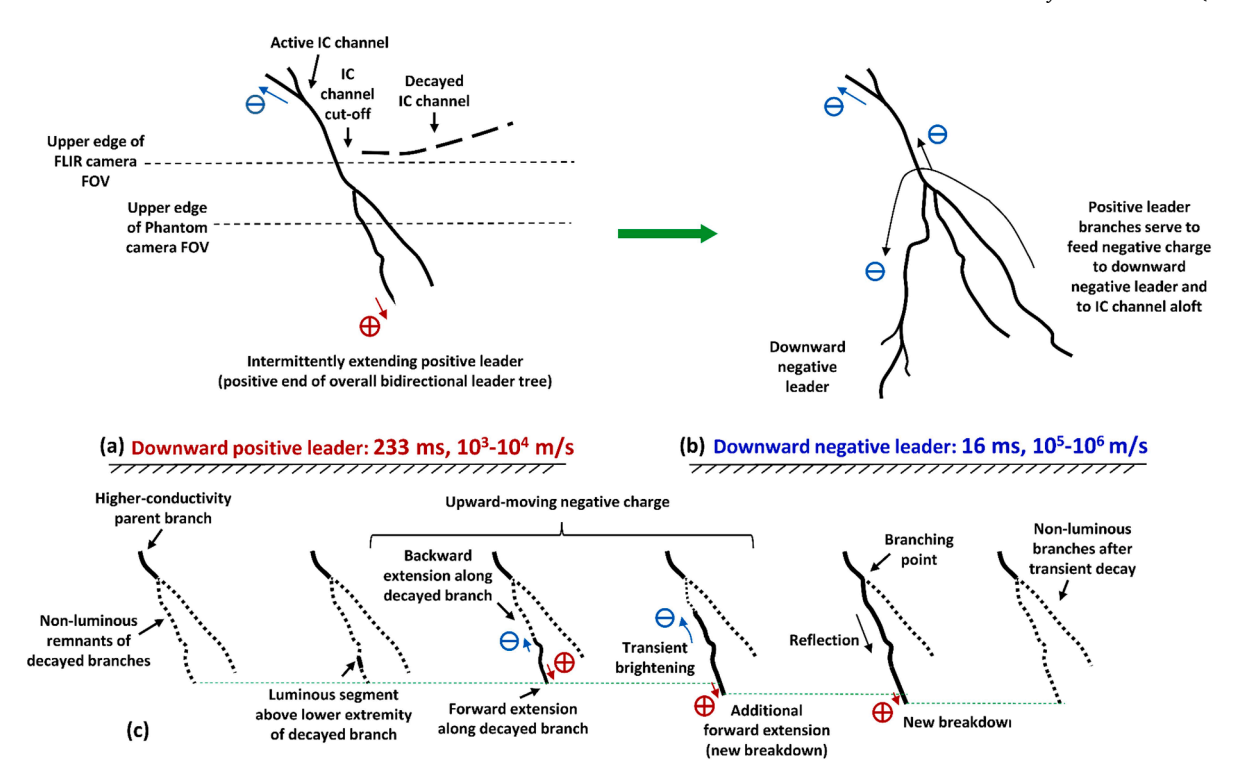


Fig. 7. Flash Z2002. Schematic representation of the key processes. (a) Overall bidirectional leader tree whose positive end was optically imaged and examined in detail in this study; (b) formation of downward negative leader that resulted in a three-stroke –CG; (c) bidirectional transient leading to forward extension of positive leader branch.

(a total of six) in that flash were initiated by bidirectional (negative end extending downward) leaders with durations of the order of 1 ms. The RS electric field waveforms in that flash were, as noted above, very similar to their counterparts in the tower-terminated -CG presented in this paper (see Fig. 2).

# 3.2. Case 2, flash Z2002: an intermittently extending downward positive leader results in a three-stroke –CG

The downward positive leader and its conversion to a negative cloudto-ground flash presented in this paper were observed in a lightning flash labeled Z2002. Leader polarity was determined from the polarity of transient electric field changes and geometry, as described in Ding et al. [33]. Flash Z2002 occurred on June 29th, 2020 at 21:47:17.880387584 UTC. It can be classified as a hybrid flash, since it started as an intracloud discharge (IC) that produced a branched downward positive leader giving rise to a negative cloud-to-ground discharge (-CG). The observed conversion could be viewed as one of the mechanisms of -CG initiation. The -CG was composed of three strokes (leader/return-stroke sequence), all of which followed the same channel to ground. According to the NLDN, the distance from the channel to ground to the LOG was 6.2 km and the magnitudes of return-stroke (RS) peak currents for the three strokes were (in the order of occurrence) 93 kA, 14 kA, and 12 kA, All three strokes of the -CG, as well as the branched positive leader (lower part of the overall bidirectional leader tree), were imaged by both Phantom (50-µs interframe interval) and FLIR (1-ms interframe interval) cameras. Selected frames showing the dynamics of positive leader (lower part of the overall bidirectional leader tree) are shown in Fig. 5a – e, and the composite image of the downward positive leader is shown in Fig. 5f. Further, the negative downward leader and the return-stroke

stage of Stroke 1 are presented in Fig. 5g and 5h, respectively. Finally, the initiation of Strokes 2 and 3 can be seen Fig. 5i and 5j, respectively.

Evolution of the downward negative leader is presented in Fig. 6, which shows 1 composite and 17 individual 1-ms FLIR frames. It initiated right after the transient in the right branch (RB) of the downward positive leader, while its left branch (LB) carried continuing current (CC), as seen in FLIR Frame -17. Only FLIR frames are shown in Fig. 6 because the initiation point of the negative leader was outside the Phantom FOV. The negative leader is first seen in Frame -16. It initially followed, at least in part, the remnants of pre-existed branch, labeled CGB in Fig. 5a and b, and then, starting with Frame -9, extended through cold air. Negative leaders in cold air always propagate in a stepped fashion, although individual steps are not resolved with our high-speed cameras. Initially, the negative leader propagated at a speed of the order of  $10^5$  m/s and then, starting with Frame -6, exhibited acceleration and significant branching. In Frames -16 to -4, the CCcarrying LB seems to be feeding both the descending negative leader and the in-cloud channel aloft (negative part of the bidirectional leader tree). In Frame −3, the link to the in-cloud channel weakens, so that LB mostly feeds the descending negative leader. In Frame -2, the link to the in-cloud channel appears to be almost completely decayed. In Frame -1, there is a transient in RB that strongly intensifies the descending negative leader (via a  $\beta_2$ -type-leader process; e.g. Schonland, [34]) and also re-establishes/enhances the decayed link to the in-cloud channel aloft. From Frame -6 to Frame -1, the IR brightness of the negative leader channel dramatically increases and its propagation speed increases by about an order of magnitude, from  $10^5$  to  $10^6$  m/s.

From the analysis of higher time resolution Phantom images, we found that the positive leader extended intermittently, via transients separated by millisecond-scale quiet intervals. We have found that the

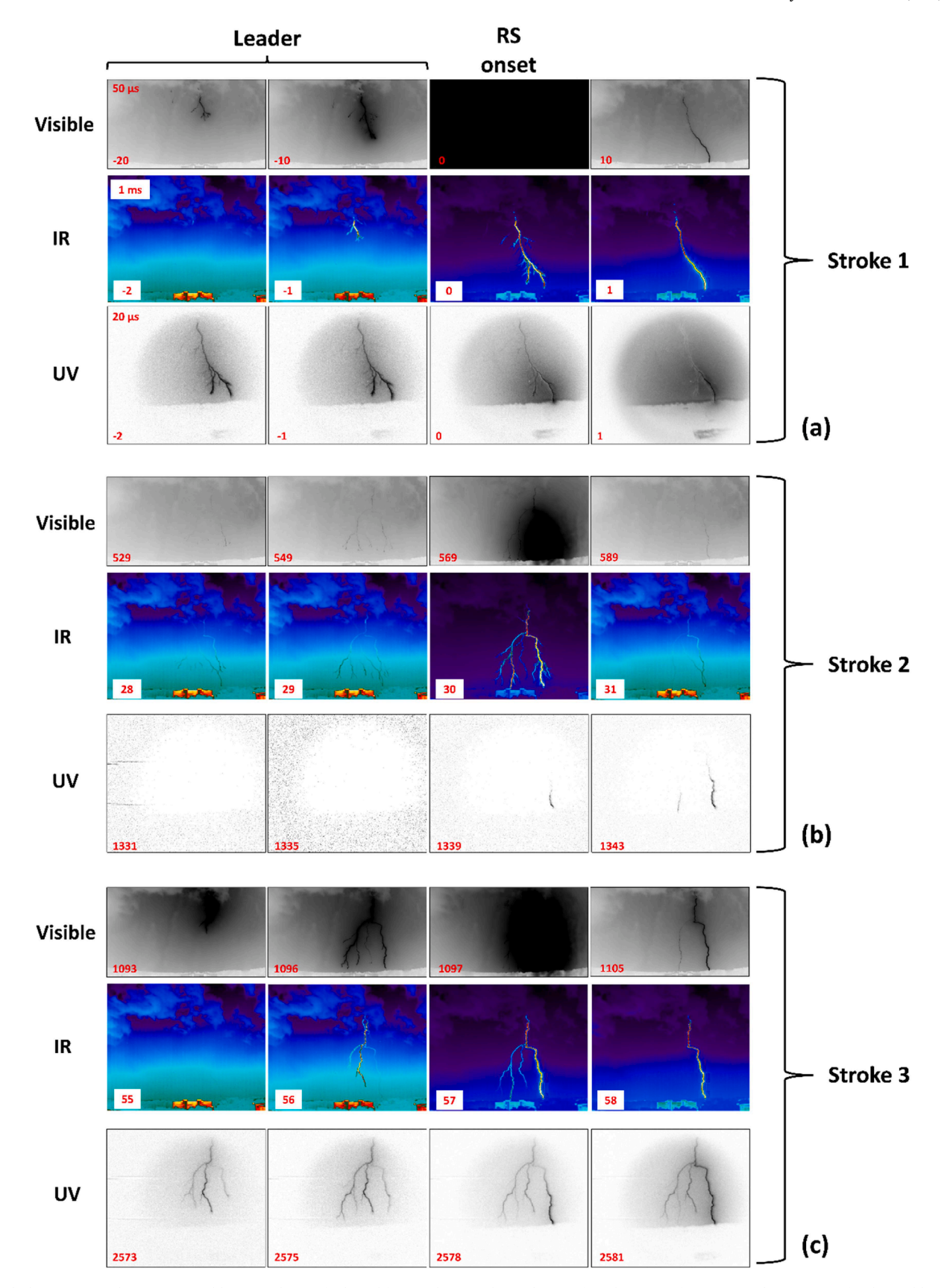
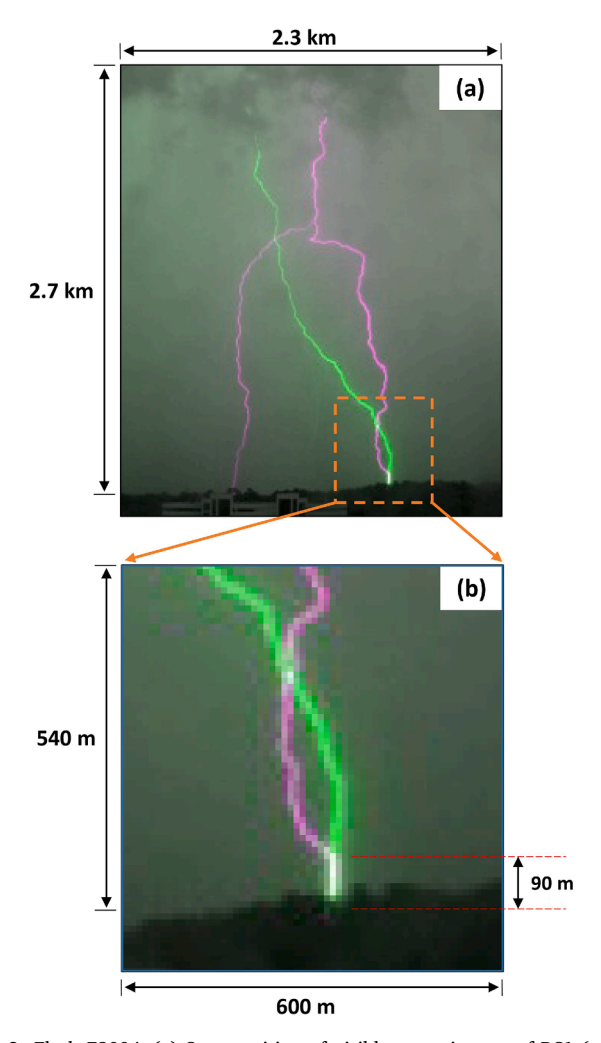


Fig. 8. Flash Z2004. (a) Three rows (Visible, IR, and UV) of selected frames showing the evolution of Stroke 1. Interframe intervals were  $50 \mu s$  for the visible, 1 ms for IR, and  $20 \mu s$  for UV. Frame numbers relative to the onset of the return-stroke (RS) stage of Stroke 1 are given in the lower-left corner of each frame. The visible-range and UV-range frames are inverted. (b) and (c) are the same as (a), but for Strokes 2 and 3, respectively. RS onset frames for Strokes 2 and 3 are approximately aligned with that of Stroke 1. The preceding and following frames are not aligned and are selected to optimize visualization of the evolution of imaged channels.



**Fig. 9.** Flash Z2004. (a) Superposition of visible-range images of RS1 (green color) and RS2 (magenta color). White color indicates channel sections that coincide in the lightning image plane. The lowest 90-m channel section, which is essentially straight and vertical, was apparently shared by RS1 and RS2. Note the second ground termination point created by the leader of Stroke 2. The two ground termination points (the same for Stroke 3) are separated by about 950 m. (b) Expansion of a portion of (a) inside the orange broken-line box.

transients (1) are mostly initiated in a previously created but already decayed branch, a few hundreds of meters above its lower extremity, (2) extend bidirectionally, (3) establish a temporary steady-current connection to the negative part of the overall bidirectional leader tree, and (4) exhibit brightening accompanied by new breakdowns at the positive end. Both positive and negative ends extended at speeds of  $10^6$  to  $10^7$  m/s, while the overall positive leader extension speed was as low as  $10^3$  to  $10^4$  m/s. Both the conversion of the downward positive leader to –CG and the dynamics of transients are schematically illustrated in Fig. 7.

3.3. Case 3, flash Z2004: heavily-branched negative leader of stroke 2 enters the residual channel of stroke 1 near ground, in addition to creating a new ground termination point

The third unusual behavior we are going to present in this paper was observed in a downward negative lightning flash labeled Z2004. Flash

Z2004 occurred on July 10th, 2020 at 23:33:15.220273408 UTC. According to the NLDN, the distance from the channel to ground to the LOG was about 5 km (5.1 km for the first and third strokes and 5.25 km for the second stroke) and the magnitudes of return-stroke (RS) peak currents for the three strokes were (in the order of occurrence), 151 kA, 13 kA, and 23 kA. Strokes 2 and 3 each produced two ground terminations, one of which was the same as the only ground termination of Stroke 1. All three strokes of the –CG were imaged in the visible (Phantom v310, 50-μs interframe interval), infrared (FLIR, 1-ms interframe interval), and ultraviolet (CoronaFinder coupled with U-340 filter and Phantom v711, 20-μs interframe interval) systems. Selected frames from all three systems for all three leader/return-stroke (L/RS) sequences (two frames for the leader stage and two frames for the RS stage) are presented in Fig. 8.

Frames 28, 29, and 31 in Fig. 8b (middle row) show the residual infrared (IR) luminosity of the channel to ground created by Stroke 1 (see Frame 1 in Fig. 8a, middle row), which is clearly different from the channel of Stroke 2 seen in Frame 30 in Fig. 8b (middle row). Note that the residual channel of Stroke 1 is non-luminous in either visible or UV records. The difference between the channels of Strokes 1 and 2 is further illustrated by a superposition of visible-range images of RS1 (green color) and RS2 (magenta color) in Fig. 9a. It appears that the right branch of the leader of Stroke 2 entered the residual channel of Stroke 1 at a height of about 90 m above ground, as shown in more detail in Fig. 10. To the best of our knowledge, such unusual behavior of a subsequent-stroke leader has never been reported before. Note that the time interval between RS1 and RS2 was relatively short, about 29 ms, and the NLDN-reported current peak for RS2 is 13 kA, more than an order of magnitude lower than 151 kA reported for RS1.

Fig. 10a shows the last visible-range 50- $\mu$ s frame (Frame 568) of the leader stage of Stroke 2, with an expansion of the portion of this leader inside the red broken-line box being presented in Fig. 10b. At least five major leader branches spanning a 2D horizontal distance of about 1.8 km and simultaneously approaching ground can be seen in Frame 568. Shown in Fig. 10c are 24 visible-range frames (the first 20 of them are consecutive and correspond to the leader of Stroke 2) of the region inside the red broken-line box in Fig. 10b (magenta color), superimposed on which is the channel of RS1 (green color). Black color corresponds to superposition of magenta on green. RS2 occurred in Frame 569. Frames 569 through 572 (spanning about 200  $\mu$ s) are saturated and not shown in Fig. 10c.

Two branches are seen in Fig. 10c to extend downward, with the left one nearly touching the ground in Frame 568, while the much fainter right branch collides with the residual channel of Stroke 1 and produces RS2, as seen in Frames 573 to 576. Those two leader branches approached the ground at similar average speeds of about  $2.2\times10^5\,\mathrm{m/s}$ , estimated from Frames 549 to 568, shown in Fig. 10c. The frame-to-frame 2D speed of the leader of Stroke 2 between Frames 568 and 569 (along the bottom 90-m section of the channel) was at least  $1.8\times10^6\,\mathrm{m/s}$ , assuming the absence of significant upward connecting leader (UCL) along the residual channel of Stroke 1. It is conceivable that there could be an undetected (due to insufficient time resolution of the camera) UCL along the residual channel, which served to attract the right branch and prevent almost imminent attachment of the left branch to ground.

# 4. Summary

We presented recent observations of very unusual behavior of lightning discharges including the following:

(a) the ability of -CG to briefly couple to a concurrent +CG many kilometers away,

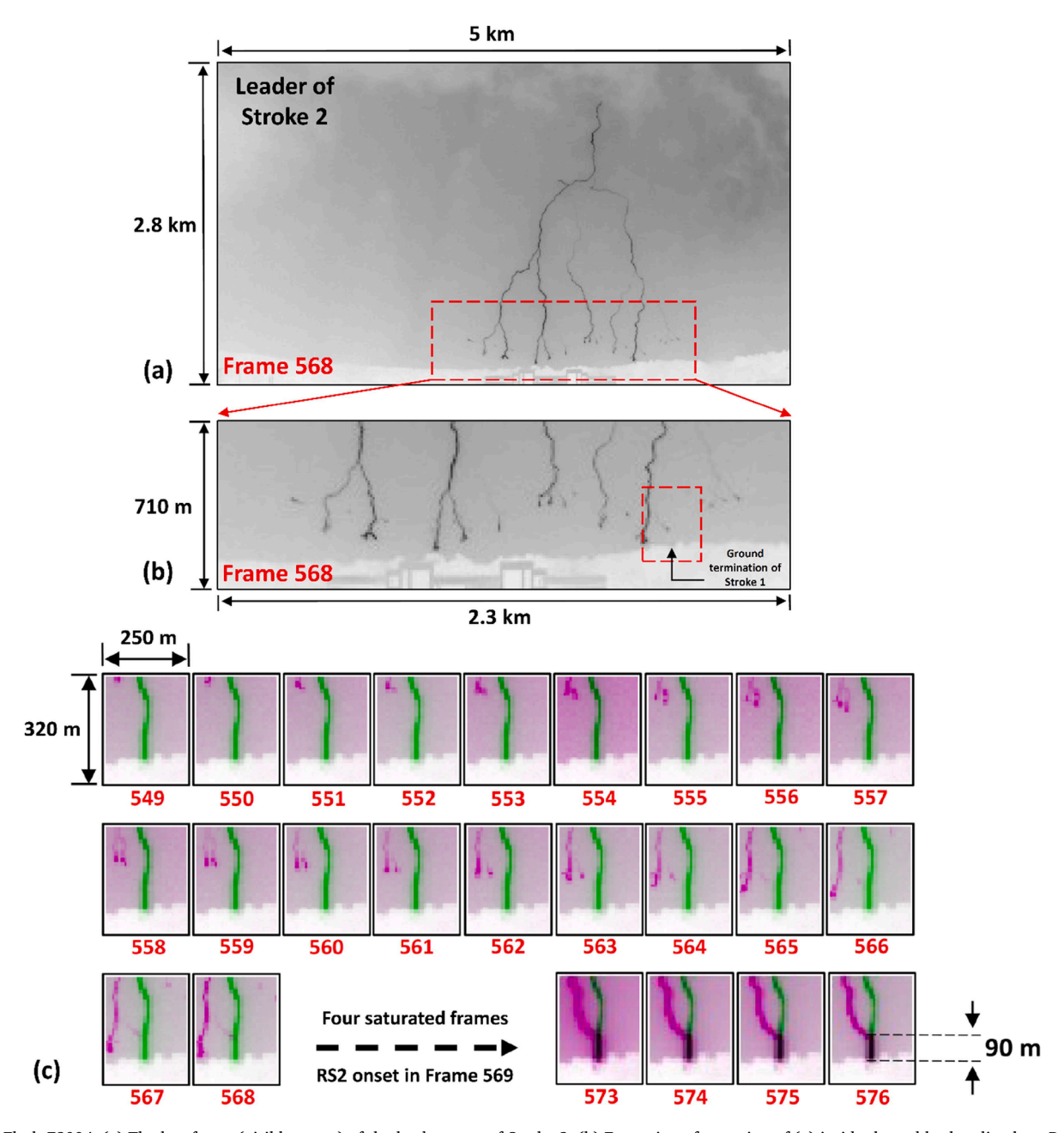


Fig. 10. Flash Z2004. (a) The last frame (visible-range) of the leader stage of Stroke 2. (b) Expansion of a portion of (a) inside the red broken-line box. Position of ground termination point is also shown. (c) Selected consecutive frames of the leader stage of Stroke 2 (magenta color) inside the red broken-line box in (b), superimposed on which is the image of the channel of RS1 (green color). Black color represents superposition of magenta on green. RS2 began in Frame 569 and saturated this and three more 50-µs frames. The saturated frames are not shown here. Note that in the original Frames 549 to 576 the RS1 channel shown in green in (c) is decayed and totally invisible.

- (b) the ability of downward positive leader to produce an opposite-polarity (negative) lightning discharge to ground (-CG), and
- (c) the ability of subsequent-stroke leader, moving through virgin air, to enter the lower part of the residual channel of the preceding stroke, in addition to creating a new ground termination point.

Clearly, further research is needed to better understand such unusual lightning behavior.

Studying unusual lightning behavior helps to improve our knowledge of the variability of basic lightning processes (still not fully understood) and to identify new potential lightning hazards to various objects and systems.

# **Funding**

This research was supported in part by NSF grant AGS-2114471.

# CRediT authorship contribution statement

**Z. Ding:** Writing – original draft, Software, Methodology, Formal analysis, Data curation, Conceptualization. **V.A. Rakov:** Writing – review & editing, Supervision, Conceptualization.

# **Declaration of competing interest**

The authors declare that they have no known competing financial interests or personal relationships that could have appeared to influence

the work reported in this paper.

# Data availability

All the data and results for Flashes Z1906, Z2002, and Z2004 can be found at: https://doi.org/10.6084/m9.figshare.24978423.v1.

# Acknowledgements

The authors would like to thank Levi Blanchette of Vaisala Inc. for providing NLDN data.

# **Appendix**

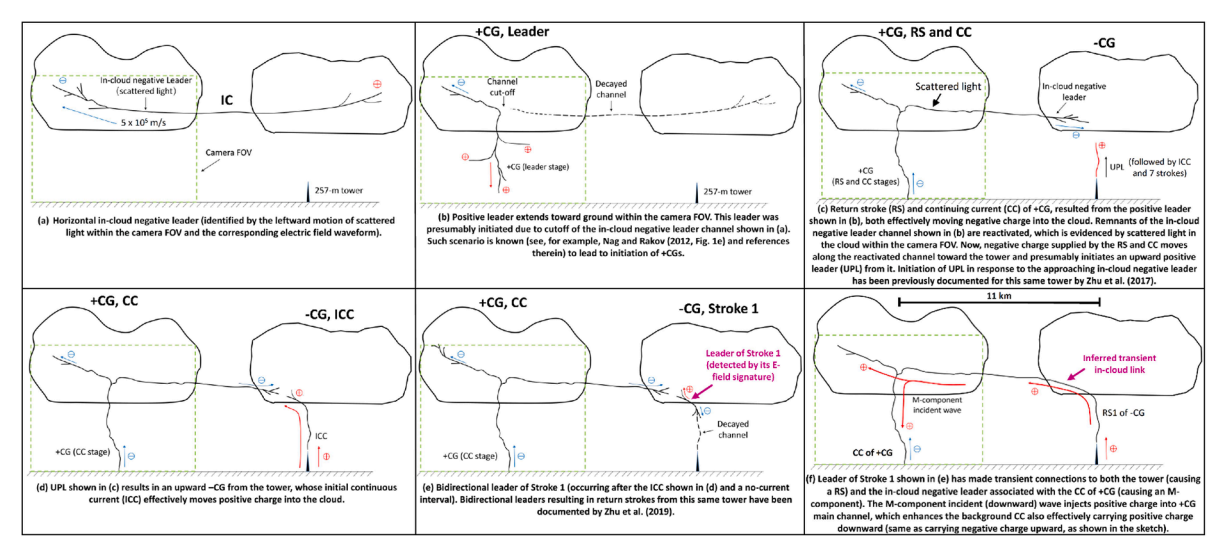


Fig. A1. Flash Z1906. Hypothetical scenario leading to establishment of a transient in-cloud link between +CG and tower-terminated -CG. Panels (e) and (f) are also shown in Fig. 4. Plus and minus signs inside small circles indicate the polarity of moving charge, with the direction of charge motion being shown by arrows. In (f), the RS current peak is expected to be strongly attenuated within the first kilometer of the channel attached to the tower, so that its contribution to the M-component current in the +CG main channel is expected to be comparable to the contribution of the preceding leader, during which the M-component started.

# References

- M.M.F. Saba, et al., High-speed video observations of positive lightning flashes to ground. J. Geophys. Res. Atmos. 115 (24) (2010) 1–9.
- [2] M.M.F. Saba, D.R.R. da Silva, J.G. Pantuso, C.L. da Silva, Close view of the lightning attachment process unveils the streamer zone fine structure, Geophys. Res. Lett. 49 (24) (2022). Dec.
- [3] T.A. Warner, M.M.F. Saba, C. Schumann, J.H. Helsdon, R.E. Orville, Observations of bidirectional lightning leader initiation and development near positive leader channels, J. Geophys. Res. Atmos. 121 (15) (2016) 9251–9260. Aug.
- [4] M.D. Tran, V.A. Rakov, Initiation and propagation of cloud-to-ground lightning observed with a high-speed video camera, Sci. Rep. 6 (December) (2016) 1–11.
- [5] M.D. Tran, V.A. Rakov, A study of the ground-attachment process in natural lightning with emphasis on its breakthrough phase, Sci. Rep. 7 (1) (2017) 1–13.
- [6] S. Visacro, M. Guimaraes, M.H. Murta Vale, Features of upward positive leaders initiated from towers in natural cloud-to-ground lightning based on simultaneous high-speed videos, measured currents, and electric fields, J. Geophys. Res. Atmos. 122 (23) (2017), 12,786-12,800.
- [7] S. Visacro, M. Guimaraes, M.H. Murta Vale, Striking distance determined from high-speed videos and measured currents in negative cloud-to-ground lightning, J. Geophys. Res. Atmos. 122 (24) (2017), 13,356-13,369.
- [8] Z. Ding, V.A. Rakov, Y. Zhu, M.D. Tran, On a possible mechanism of reactivation of decayed branches of negative stepped leaders, J. Geophys. Res. Atmos. 125 (23) (2020) 1–17.
- [9] Z. Ding, V.A. Rakov, Y. Zhu, M.D. Tran, A.Y. Kostinskiy, I. Kereszy, Evidence and inferred mechanism of collisions of downward stepped-leader branches in negative lightning, Geophys. Res. Lett. 48 (11) (2021) 1–9.
- [10] A. Nag, et al., Characteristics of upward-connecting-leader current leading to attachment in downward negative cloud-to-ground lightning strokes, Atmos. Res. 294 (July) (2023) 106943.
- [11] B. Wu, et al., High-Speed video observations of recoil leaders producing and not producing return strokes in a canton-tower upward flash, Geophys. Res. Lett. 46 (14) (2019) 8546–8553.
- [12] B. Wu, et al., High-Speed video observations of needles evolving into negative leaders in a positive cloud-to-ground lightning flash, J. Geophys. Res. Atmos. 128 (21) (2023).
- [13] W. Rison, et al., Observations of narrow bipolar events reveal how lightning is initiated in thunderstorms, Nat. Commun. 7 (2016).

- [14] M.G. Stock, et al., Continuous broadband digital interferometry of lightning using a generalized cross-correlation algorithm, J. Geophys. Res. 119 (6) (2014) 3134–3165.
- [15] O.A. van der Velde, J. Montanyà, S. Soula, N. Pineda, J. Mlynarczyk, Bidirectional leader development in sprite-producing positive cloud-to-ground flashes: origins and characteristics of positive and negative leaders, J. Geophys. Res. Atmos. 119 (22) (2014) 238. Nov.
- [16] R. Jiang, et al., Channel branching and zigzagging in negative cloud-to-ground lightning, Sci. Rep. 7 (1) (2017) 1–9.
- [17] R. Jiang, et al., Fine structure of the breakthrough phase of the attachment process in a natural lightning flash, Geophys. Res. Lett. 48 (6) (2021) 1–9.
- [18] B.M. Hare, et al., Needle-like structures discovered on positively charged lightning branches, Nature 568 (7752) (2019) 360–363.
- [19] Y. Pu, S.A. Cummer, Needles and lightning leader dynamics imaged with 100–200 MHz broadband VHF interferometry, Geophys. Res. Lett. 46 (22) (2019) 13556–13563.
- [20] D.P. Jensen, X.-M. Shao, R.G. Sonnenfeld, Insights into lightning k-leader initiation and development from three dimensional broadband interferometric observations, J. Geophys. Res. Atmos. 128 (23) (2023) 1–24. Dec.
- [21] S. Yuan, R. Jiang, X. Qie, Z. Sun, D. Wang, A. Srivastava, Development of side bidirectional leader and its effect on channel branching of the progressing positive leader of lightning, Geophys. Res. Lett. 46 (3) (2019) 1746–1753.
- [22] S. Yuan, R. Jiang, X. Qie, D. Wang, Side discharges from the active negative leaders in a positive cloud-to-ground lightning flash, Geophys. Res. Lett. 48 (17) (2021) 1–12.
- [23] R. Jiang, S. Yuan, X. Qie, M. Liu, D. Wang, Activation of abundant recoil leaders and their promotion effect on the negative-end breakdown in an intracloud lightning flash, Geophys. Res. Lett. 49 (1) (2022).
- [24] Y. Zhu, W. Lyu, J. Cramer, V. Rakov, P. Bitzer, Z. Ding, Analysis of location errors of the U.S. national lightning detection network using lightning strikes to towers, J. Geophys. Res. Atmos. 125 (9) (2020).
- [25] V.A. Rakov and M.A. Uman, "Lightning: physics and Effects Vladimir A. Rakov, Martin A. Uman - Google Books," Cambridge, 2003.
- [26] V.A. Rakov, S. Mallick, A. Nag, V.B. Somu, Lightning Observatory in Gainesville (LOG), Florida: a review of recent results, Electr. Power Syst. Res. 113 (2014) 95–103.
- [27] V.A. Rakov, et al., High-Speed optical imaging of lightning and sparks: some recent results, IEEJ Trans. Power Energy 138 (5) (2018) 321–326. May.

- [28] V.A. Rakov, et al., New insights into the lightning discharge processes, Plasma Sources Sci. Technol. 31 (10) (2022) 104005.
- [29] Z. Ding, Rakov, Toward a better understanding of negative lightning stepped leaders, Electr. Power Syst. Res. 209 (2022) 108043.
- [30] Y. Zhu, V.A. Rakov, M.D. Tran, Optical and electric field signatures of lightning interaction with a 257-m tall tower in Florida, Electr. Power Syst. Res. 153 (2017) 128–137
- [31] Y. Zhu, V.A. Rakov, M.D. Tran, W. Lyu, D.D. Micu, A modeling study of narrow electric field signatures produced by lightning strikes to tall towers, J. Geophys. Res. Atmos. 123 (18) (2018), 10,260-10,277.
- [32] Z. Ding, V.A. Rakov, Y. Zhu, M.D. Tran, I. Kereszy, Transient phenomena in positive cloud-to-ground lightning discharges, Commun. Phys. 5 (1) (2022) 1–12.
   [33] Z. Ding, V.A. Rakov, Y. Zhu, I. Kereszy, S. Chen, M.D. Tran, Propagation
- [33] Z. Ding, V.A. Rakov, Y. Zhu, I. Kereszy, S. Chen, M.D. Tran, Propagation mechanism of branched downward positive leader resulting in a negative cloud-toground flash, J. Geophys. Res. Atmos. 129 (1) (2024). Jan.
- [34] B.F.J. Schonland, Progressive lightning. IV. The discharge mechanism, Proc. R. Soc. Ser. A, Math. Phys. Sci. 164 (1938) 132–150.